

Bipartite Relativistic Quantum Information from Effective Field Theory Approach with Implications to Contextual Meanings of Locality and Quantumness

Feng-Li Lin^a and Sayid Mondal^b

^a*Department of Physics, National Taiwan Normal University, Taipei, 11677, Taiwan*

^b*Instituto de Ciencias Exactas y Naturales,*

Universidad Arturo Prat, Playa Brava 3256, 1111346, Iquique, Chile

E-mail: fengli.lin@gmail.com , sayid.mondal@gmail.com

Abstract

In a recent work [1], the effective field theory (EFT) is adopted to consider the quantum decoherence of a near-horizon Unruh-DeWitt (UDW) charged qubit in a macroscopic cat state. We generalize this EFT approach to study the relativistic quantum information (RQI) of two static UDW-charged qubits with or without a black hole. This EFT is obtained by integrating out a massless mediator field, yielding the direct Coulombic interactions among intrinsic multipole moments of UDW detectors and the induced one on the black hole. The RQI of the quantum state of the mediator field can be probed by the reduced final states of UDW detectors by tracing out the induced internal states of the black hole. From the reduced final state, we find the patterns of entanglement harvesting agree with the ones obtained by the conventional approach based on master theory. However, the more detailed study suggests that the contextual meanings of (non-)locality may or may not be the same in quantum field theory (QFT) and RQI. To explore the contextual meanings of quantumness and locality more, we also calculate quantum discord and locality bound of the Bell-type experiments, with the former characterizing the non-classical correlations and the latter the (non-)locality in the hidden-variable context of RQI. We find that QFT and RQI agree on quantumness based on different physical reasons but may not agree on locality.

Contents

1	Introduction	2
2	EFT for UDW Detectors and Blackbody	6
3	Reduced States of UDW detectors	9
3.1	Case I: Without black hole	10
3.2	Case II: Neglecting direct interaction between UDW detectors	11
3.3	Case III: Including all direct interactions	13
3.4	Features of reduced final states and RQI measures	13
4	Entanglement Harvesting	15
4.1	Case I	15
4.2	Case II	16
4.3	Case III	16
4.3.1	Configuration a	17
4.3.2	Configuration b	18
4.3.3	Configuration c	18
5	Quantum Discord	19
5.1	Case I	20
5.2	Case II and III	20
5.2.1	Configuration a	20
5.2.2	Configuration b	21
6	Nonlocality Bound	21
6.1	Case I	22
6.2	Case II	23
6.2.1	Configuration a	23
6.2.2	Configuration b	24
6.3	Case III	24
6.3.1	Configuration a	25
6.3.2	Configuration b	25
7	Conclusion and Discussions: Contextual meanings of locality and quantum-ness	26

1 Introduction

Relativistic quantum information (RQI) has been proposed [2–4] over two decades to study how the novel discoveries of quantum fields on the curved spacetime, such as Hawking radiation and Unruh effect, will introduce nontrivial effects in the usual protocols and tasks in the quantum

information and quantum communication, such as teleportation [5–7], quantum decoherence [8–12], entanglement harvesting [13–21], etc. It can be thought of as incorporating the general and special relativistic effects into the quantum channels for quantum computing and communication. In particular, the relativistic causality and the thermal nature of spacetime with event horizons turn the relativistic effects into the new ingredients for the quantum channels.

The typical setup for RQI is to consider the Unruh-DeWitt (UDW) detectors interacting with the environmental quantum fields on nontrivial curved backgrounds such as black holes, Rindler spacetime, or de Sitter space. One can then evolve the whole system and find the reduced final states of the UDW detector to extract the relevant quantum information. For this kind of consideration, most quantum information probed by the reduced final states is encoded in the spectral function of the environmental quantum field. However, due to complications of the background metric, the spectral function and the reduced states may not have analytical forms. Moreover, the numerical calculation of the reduced final state will also be plagued by the infinite number of poles associated with the thermal-like nature of the background spacetime and may result in inaccuracy. This will hinder an intuitive understanding of the results based on numerical analysis.

In the above-mentioned approach, all the entities except the black hole treated as background, such as UDW detectors with internal spins, interact via their multipole moments with the environmental quantum field thermalized by the event horizon of the black hole. In a sense, all the entities are immersed in the environmental field thermalized by the black hole. The results are then summarized and encoded in the environmental field’s spectral two-point function, which appears in the reduced final states of UDW detectors’ quantum spins. Usually, the spectral two-point function of a quantum field without self-interactions behaves like a classical field in flat spacetime. In the presence of a black hole background, its event horizon will induce the nontrivial quantum effect of the scalar field and turn its free spectral function into a related thermal one. Thus, the mediator behaves almost as a classical thermal field. With this understanding, one may try to overcome the above difficulty using the effective field theory (EFT) approach. The EFT is a low-energy approximation of the master field theory. All entities, including black holes, should have tiny sizes compared to the inter-distances among them for the EFT to be valid. With such a scale hierarchy, one can integrate the hard modes of the mediator quantum field to arrive at an effective action for all particle-like entities interacting directly with each other via interactions sourced by their multipole moments. These direct interactions may couple the (quantum) spins non-locally and yield the nontrivial reduced final states of UDW detectors. We compare the two approaches in fig. 1.

Let us elaborate more on the advantages of the EFT approach to obtain the final reduced states of UDW detectors, which act as the probe to extract the RQI of the underlying quantum field in nontrivial background spacetime. One immediate advantage is that black holes are now on the same footing as the UDW detectors as the point-like particles with internal degrees of freedom. Augmented with the kinetic energies of particle-like entities in the EFT, one can consider the

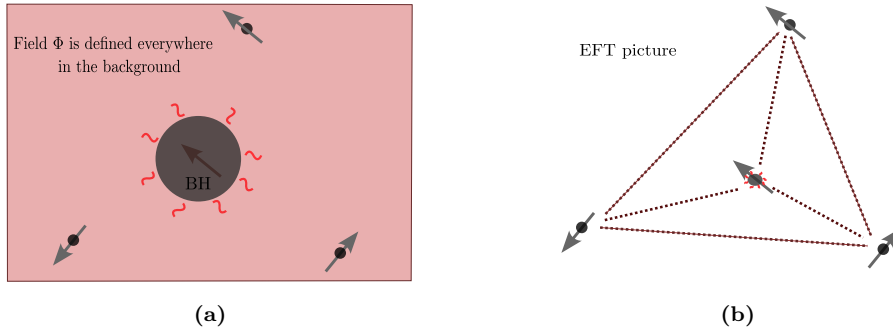


Figure 1: Comparison of the conventional approach based on master theory and the approach of its EFT for the problems of RQI. In the EFT, the black hole becomes point-like but possesses multipole moments induced by the dynamical modes of the environmental field Φ . All the entities are held static and interact directly via Coulombic forces sourced by their multipole moments. On the other hand, in the master theory, the black hole is a spacetime background, which thermalizes Φ .

reduced final states of any entities in the dynamical setting, including the back-kick effects from radiation reaction to the final reduced states. Moreover, if the mediator field is massless, the direct interaction is just the long-ranged Coulomb-like forces acting on the corresponding multipole moments of the participating entities held steadily. One can extend the above leading effective action by the velocity expansion to obtain the post-Newtonian (PN) style EFT [22–24]. The interactions in the PN EFT are spooky because they non-locally couple the internal quantum spins of UDW detectors, which may yield non-local resources such as quantum entanglement for the quantum information tasks. This indicates the EFT approach can be adopted as a framework for RQI.

The second advantage is more subtle and less noticeable. In the above setup, we have endowed the UDW detectors with multipole moments of the environmental field by hand to interact with each other via the mediator field. However, it is less clear how we can endow the black holes with the multipole moments of the environmental field. This is because the no-hair theorem of black holes usually does not allow these multipole moments. Intuitively, the no-hair theorem implies that the black hole is a rigid body so that its shape cannot be tidally deformed by the environmental field. This is indeed true if the environmental field is static [25–30]. However, a black hole can be tidally deformed by a dynamical environmental field, which is characterized by the dynamical tidal Love number (TLN). Moreover, by the decoupling theorem [31, 32], the dynamical TLN at the low-energy regime is linear in frequency and is universal [28, 33–35], i.e., independent of the high-energy theory of the environmental field and quantum gravity. Thus, the internal multipole moments associated with the particle-like black holes are nothing but the ones induced by the universal dynamical tidal deformation. Due to no hair theorem, these tidal deformations should be unstable, and so are the induced multipole moments. The instability is characterized by the nonzero imaginary part of the corresponding TLNs. However, the dynamical tidal deformation is purely a classical feature of a black hole under a classical environmental field and by itself cannot capture the black hole’s quantum aspect, such as Hawking radiation.

Motivated by the problem of the induced quantum decoherence of a which-path qubit by the

black hole's event horizon proposed in [9, 10], the authors of [1] devised the EFT approach to tackle it. By exploiting the aforementioned advantages and combining the dynamical tidal effect and the thermal nature of the near-horizon environmental field, they arrive at a result in agreement with the one obtained from the conventional approach using master field theory [9–11]. Inspired by the EFT's success of [1], we generalize the EFT approach to consider the bipartite RQI in this paper. That is, we consider two spatially separated static UDW detectors, each of which possesses an internal qubit. These particle-like UDW detectors also carry multipole moments of the environmental field thermalized by the event horizon of a background black hole. For comparison with the quantities obtained by the conventional master theory approach, we will use the EFT to compute the entanglement harvesting [15, 16] by the UDW detectors from the environmental field. As expected, we can reproduce the patterns of entanglement harvesting obtained by the conventional master theory approach as in [16]. However, with the EFT approach, we can obtain almost all the results in the analytical form. More importantly, we can see how the different interaction terms in the EFT affect the pattern of the entanglement harvesting. For example, if we neglect the direct interaction between the multipole moments of two UDW detectors, the remaining direct interactions between the UDW detectors and the black hole will always yield no entanglement harvesting. This seems counter-intuitive, but it is what is predicted by EFT. Besides entanglement harvesting, we also consider quantum discord and nonlocality bound of Bell's type experiments to characterize the RQI nature of each interaction term in EFT. The quantum discord [36, 37] characterizes pure quantum correlation, thus, the quantumness of the bipartite states. The nonlocality bound [38–40], on the other hand, is to examine if any EFT interaction, such as the spooky Coulombic force, is nonlocal to violate the Bell-like inequality. Based on our results, our understanding of important concepts such as quantumness and (non-)locality may have opposite meanings in different contexts, e.g., quantum field theory and quantum information. We will elaborate more on this interesting contrast in the concluding section of this paper.

The remainder of the paper is organized as follows. In the next section section 2, we sketch the EFT for UDW detectors with internal quantum spins interacting mutually and with the black hole (or some blackbody) via a massless mediator field. In section 3, we derive the reduced final states for the quantum spins of the UDW detectors by tracing out the black hole's internal degrees of freedom due to thermal effect and tidal deformations. The result can be approximated in the low-energy regime as a simple expression proportional to the zero-frequency limit of spectral density. In section 4, we use these reduced final states to evaluate concurrence to quantify entanglement harvesting for three cases: (1) without the black hole, (2) neglecting the direct interaction between UDW detectors, and (3) including both (1) and (2). For each case, we consider two or three configurations of spatial positions of the entities. In (3), we recover the characteristics of concurrence obtained from the conventional approach. In section 5 and 6, we consider the above cases and configurations for quantum discord and bipartite nonlocality bound, respectively. Finally, we conclude our paper in section 7 on the contextual meaning of

locality and quantumness.

2 EFT for UDW Detectors and Blackbody

In this section, we review and extend the EFT approach of [1] to incorporate the interaction between the UDW detectors and a blackbody via an ambient mediator field. Such a blackbody can be a quantum black hole or a generic blackbody at a fixed temperature. Based on this formulation, we would like to study the entanglement harvesting and quantum correlation of the pair of UDW detectors.

We consider the UDW detectors and the blackbody with multipole moments denoted by Q_i^I with I as the tensor index characterizing the multipole moments and $i = 1, 2, B$ labeling the two UDW detectors and the blackbody, respectively. These multipole moments Q_i^I 's source and interact with each other via the corresponding ambient massless tensor fields Φ_I 's. Moreover, the blackbody is a quantum object, therefore Q_B^I 's are quantum operators, and their spectral properties dictate the time evolution. However, for simplicity, we treat $Q_{1,2}^I$ as classical quantities. Besides the multipole moment, the UDW detector can also possess internal quantum spin $J_{a=1,2}$ acting on the associated spin Hilbert space $\mathcal{H}_{a=1,2}^S$. For example, we can think of the UDW detector as some realistic atom that carries both the quantum (iso)spin and the multipole moment interacting with the Maxwell field. Similarly, the blackbody can also own quantum spin denoted by J_B , formed from the coherent fermion condensation. A black hole with quantum spin is not a Kerr black hole with classical angular momentum due to the self-rotation.

At low energy, the dynamics of the above system can be described by the following EFT action

$$S = S_{\text{Blackbody}} + \frac{1}{g_I^2} S_{\Phi} + S_{\text{UDW}} + \sum_I \int dt \Phi_I(t) \sum_{i=1,2,B} Q_i^I(t) \otimes J_i(t). \quad (2.1)$$

First, $S_{\text{Blackbody}}$ and S_{UDW} are the kinetic actions of the point-like blackbody and UDW detectors respectively. In this paper, we will only consider the static cases so that they will not play a role in this paper. Then, $\frac{1}{g_I^2} S_{\Phi}$ is the kinetic action for the ambient mediator field Φ_I . We adopt the convention in [1] by normalizing it by the square of the dimensionless universal coupling constant g_I . In this paper, we will consider only massless fields Φ_I , e.g., the scalar field of coupling constant g_0 , the Maxwell field of g_1 being the fine structure constant, and Einstein's gravity field of $g_2 := \frac{G_N}{R^2}$ with G_N the Newton's constant and R the typical size of the blackbody. The last term of (2.1) encodes the interactions between Φ_I and the multipole moment Q_i^I and the auxiliary internal quantum spin J_i . This interaction will be essential in extracting RQI from the vacuum states of Φ_I by UDW detectors' quantum spins.

We can integrate out the ambient fields to induce direct interaction among the multipole-moment operators of the same type. Moreover, due to the masslessness nature of Φ_I , after subtracting the self-energy part, the leading post-Newtonian (PN) effective action is [24]

$$S_{\text{EFT}} = \sum_I g_I \int dt \left[\sum_{a=1,2} O_{aB}^I(t) J_a(t) \otimes J_B(t) + O_{12}^I(t) J_1(t) \otimes J_2(t) \right]. \quad (2.2)$$

We see that the quantum spins of different entities now interact with each other directly. Note that the entities are in spacelike separations, so the interactions between their J_i are spooky.

Before we explain the details of the effective coupling operators $O_{ij}^I(t)$'s in (2.2), we shall give general comments about the PN EFT. The action (2.2) is just the leading term in the PN approach to the EFT by integrating out the massless mediator field [22–24]. This zeroth-order PN (0PN) action is instantaneous and Coulombic due to integrating out the hard potential mode of the mediator field. This force is off-shell because the involved entities are held statically and do not follow their geodesics. To consider the freely moving entities, we shall include the higher PN corrections in the velocity expansion. For example, the 1PN effective action in gravity is the famous Einstein-Infeld-Hoffman action [41]. With such EFT, which can also include radiation reactions at half-integral PN orders, one can study the RQI for moving UDW detectors and black holes in full dynamic aspect. However, as a preliminary study, we will only focus on the leading EFT action of (2.2).

The key ingredient of (2.2) is dictated by the effective coupling operators $O_{ij}^I(t)$'s, which are given by

$$O_{ij}^I(t) := \frac{Q_i^{I_1} N_{I_1 I_2}(\hat{r}_{ij}) Q_j^{I_2}}{r_{ij}^{2I+1}}, \quad i, j = 1, 2, B, \quad (2.3)$$

where I_1 and I_2 are two different sets of the type I indices, and the distance vectors

$$\vec{r}_{ij} := r_{ij} \hat{r}_{ij} = \vec{r}_i - \vec{r}_j, \quad \text{with} \quad |\hat{r}_{ij}| = 1. \quad (2.4)$$

The multipole-moment structure tensor $N^{I,I'}$ for the monopole, dipole, and quadrupole are given respectively by [1]

$$N(\hat{r}) = 1, \quad (2.5)$$

$$N_{i,j}(\hat{r}) = \delta_{ij} - 3\hat{r}_i \hat{r}_j, \quad (2.6)$$

$$N_{ij,kl}(\hat{r}) = 2\delta_{ik}\delta_{jl} + 35\hat{r}_i \hat{r}_j \hat{r}_k \hat{r}_l - 20\hat{r}_i \delta_{jk} \hat{r}_l. \quad (2.7)$$

For simplicity, we only consider the interactions of the same tensor types by assuming the correlators among different tensor types are negligible. Moreover, for the EFT of (2.1) to be valid, we shall assume

$$\bar{r}_i \ll r_{aB} \ll T, \quad a = 1, 2, \quad i = 1, 2, B, \quad (2.8)$$

where \bar{r}_i is the typical size of the blackbody or UDW detectors, and T is the duration of interaction between UDW detectors and the blackbody.

In the above, the multipole moments Q_B^I 's of the blackbody can be either intrinsic or extrinsically induced by the source fields Φ_I . However, if the blackbody is a black hole, it seems hard to understand such multipole moments as the intrinsic quantities due to the no-hair theorem. This raises the question of whether the multipole moments can be extrinsically induced by tidal deformation due to the ambient fields. The answer seems no, as it is known that the black

holes cannot be tidally deformed. However, this is true only for static ambient fields and not for dynamic ones. Thus, Q_B^I can be understood as the multipole moments induced by the dynamical Φ_I , so that they are related by the linear response relation characterized by the dynamical tidal Love number (TLN).

From now on, we will consider only the extrinsic Q_B^I for either a blackbody or a black hole. In such a case, the linear response relation between Q_B^I and Φ_I in the frequency domain is just the Kubo formula [42, 43] for the tidal deformation,

$$\langle Q_B^{I_1}(\omega) \rangle_\Phi = \chi^{I_2 I_1}(\omega) \Phi_{I_2}(\omega), \quad (2.9)$$

where the response function $\chi^{I_1 I_2}(\omega)$ is the Fourier transform of the retarded Green function¹

$$G_R^{I_1 I_2}(t) = -i\Theta(t) \langle [Q_B^{I_1}(t), Q_B^{I_2}(0)] \rangle. \quad (2.10)$$

If the blackbody is in a thermal state ρ_B of inverse temperature β , e.g., the Hartle-Hawking state when considering a quantum black hole, then the imaginary part of $\chi^{I_1 I_2}(\omega)$ is the dissipation kernel due to thermal or quantum transport. By the Kubo-Martin-Schwinger (KMS) condition [42, 44] on the thermal state, it leads to the fluctuation-dissipation theorem:

$$S^{I_1 I_2}(\omega) = -2(n_b(\omega) + 1) \text{Im} \chi^{I_1 I_2}(\omega), \quad n_b(\omega) = \frac{1}{e^{\beta\omega} - 1}. \quad (2.11)$$

where the fluctuation kernel $S^{I_1 I_2}(\omega)$ is the spectral density of Q_B^I defined by

$$S^{I_1 I_2}(\omega) := \int_{-\infty}^{\infty} dt e^{i\omega t} \langle Q_B^{I_1}(t) Q_B^{I_2}(0) \rangle, \quad (2.12)$$

with the Wightman function

$$\langle Q_B^{I_1}(t) Q_B^{I_2}(0) \rangle := \text{Tr}_B [\rho_B Q_B^{I_1}(t) Q_B^{I_2}(0)]. \quad (2.13)$$

At low energy, $\chi(\omega)$ manifests a universal form (see the extensive checks in [1]) as follows

$$\chi^{I_1 I_2}(\omega) = \left[A^{I_1 I_2} + \mathcal{O}((\beta\omega)^2) \right] - i \left[B^{I_1 I_2} \beta\omega + \mathcal{O}((\beta\omega)^3) \right], \quad (2.14)$$

with $A^{I_1 I_2}$ real and $B^{I_1 I_2} > 0$, and their detailed expression depends on the blackbody and the ambient fields. The positivity $B^{I_1 I_2}$ is a signature of the dissipative transport. From (2.11), this then implies that

$$S^{I_1 I_2}(\omega) = B^{I_1 I_2} (2 + \beta\omega) + \mathcal{O}((\beta\omega)^2). \quad (2.15)$$

In the case of the black hole, $A^{I_1 I_2}$ and $B^{I_1 I_2}$ are nothing but, respectively, the static and dynamical TLNs, which can be determined by the linearized field equation of Φ_I around the black hole spacetime [28, 33–35]. By imposing the ingoing condition at the horizon for the radial solution $\Phi_I(r)$, one can determine the ratio between the coefficients of $1/r^{I+1}$ and r^I terms at

¹Note that our convention for the retarded Green function differs from the one used in [1] by an overall minus sign, so that the fluctuation-dissipation relation (2.11) also differs by a sign accordingly, similarly for the minus sign in front of $B^{I_1 I_2}$ of (2.14) to take care of the convention difference.

$r \rightarrow \infty$ to yield the TLNs. The result gives $A^{I_1 I_2} = 0$ and $B^{I_1 I_2}$'s take the form for a black hole with radius r_B ,

$$B = c_0 \frac{r_B}{g_0}, \quad B^{ij} = c_1 \frac{r_B^3}{g_1} \delta^{ij}, \quad B^{ijkl} = c_2 \frac{r_B^5}{g_2} \left(\delta^{ik} \delta^{jl} + \delta^{il} \delta^{jk} - \frac{2}{3} \delta^{ij} \delta^{kl} \right), \quad (2.16)$$

where $c_{0,1,2}$ are some $\mathcal{O}(1)$ constants determined by the black hole background². However, their values will not affect the qualitative results obtained in this paper.

We shall point out an important property that $S^{I_1 I_2}(0)$ is non-vanishing if $B^{I_1 I_2} \neq 0$. This implies there is a finite portion of zero modes, which can help to facilitate the transport of RQI and yield the nontrivial reduced final states of UDW detectors, as we will see later on. From (2.14), we notice that the dissipation kernel $\text{Im} \chi^{I_1 I_2}(0) = 0$. However, due to the appearance of $n_b(\omega)$ in (2.11), and the fact that $n_b(\omega) \sim \frac{1}{\beta \omega}$ as $\omega \rightarrow 0$, one then have $S^{I_1 I_2}(0) = 2B^{I_1 I_2}$. In the case of the black hole, this combines the classical tidal deformation and the quantum effect of Hawking radiation.

3 Reduced States of UDW detectors

To study the RQI of the static UDW detectors influenced by the ambient field thermalized by the blackbody, we start with an initial state $\rho^i = \rho_{12}^i \otimes \rho_B$ with ρ_{12}^i a pure product state in $\bigotimes_{a=1,2} \mathcal{H}_a^S$ for the quantum spins of UDW detectors and ρ_B the blackbody's thermal state. The thermality of the black hole is due to the quantum effect of Φ_I in a curved background, i.e., Hawking radiation. In EFT, this thermal feature is inherited by ρ_B and encoded in the spectral density $S^{I_1 I_2}(\omega)$.

The reduced final state of the UDW detectors for their lifetimes of the whole worldlines can be obtained by

$$\rho_{12}^f = \text{Tr}_B \left[U_{w_T} (\rho_{12}^i \otimes \rho_B) U_{w_T}^\dagger \right], \quad (3.1)$$

with the evolution operator in the interaction picture constructed from the EFT action (2.2):

$$U_{w_T} = \mathcal{T} e^{-i \sum_I g_I \int_{-\infty}^{\infty} dt w_T^I(t) \left[\sum_{a=1,2} O_{aB}^I(t) J_a(t) \otimes J_B(t) + O_{12}^I(t) J_1(t) \otimes J_2(t) \right]}, \quad (3.2)$$

where $w_T^I(t)$ is a window function with an effective time interval T , i.e., $\int_{-\infty}^{\infty} |w_T^I(t)|^2 dt = T$, to characterize the turn-on profile of the type- I interaction. It is conventionally chosen as Gaussian or window type for some time interval during which the interaction is effectively switched on. It is important to note that We require T to satisfy (2.8) for the EFT to be valid.

To proceed further, we choose a specific setup to simplify the calculation while maintaining the key ingredients. We consider no quantum spin for the blackbody and choose the UDW detectors as identical two-level qubits with the energy gap Ω , that is

$$J_a = e^{i\Omega t} \sigma_a^+ + e^{-i\Omega t} \sigma_a^-, \quad (3.3)$$

where $\sigma_a^+ |0\rangle_a = |1\rangle_a$, $\sigma_a^- |1\rangle_a = |0\rangle_a$ and $(\sigma_a^+)^2 = (\sigma_a^-)^2 = 0$ for $a = 1, 2$.

²For example, for a Schwarzschild black hole with the Hawking temperature $\beta = 4\pi r_B$, $c_0 = 1$, $c_1 = \frac{1}{6}$ and $c_2 = \frac{1}{360\pi}$ [1, 28, 33, 45–47]. Note that these coefficients may slightly differ from the ones in the literature due to the different conventions adopted for the fundamental units.

3.1 Case I: Without black hole

We first consider a seemingly trivial case, that is when there is no blackbody around. Consequently, the EFT yields the Coulombic force by treating Φ_I as a classical field. We then wonder if this seemingly classical environment can yield reduced final states with nontrivial RQI, such as the entangled states. If the answer is yes, then the ‘‘classical’’ environment in the EFT will be different from the local operations and classical communications (LOCC) in the tasks of quantum communication, which cannot create quantum entanglement. This could suggest that the meaning of being classical is context-dependent.

The evolution operator (3.2) of a specific type I in this case is reduced to

$$U_{w_T} = \mathcal{T} e^{-ig_I \int_{-\infty}^{\infty} dt w_T(t) O_{12}^I(t) J_1(t) \otimes J_2(t)} , \quad (3.4)$$

and the reduced final state takes the form

$$\rho_{12}^f = \begin{pmatrix} 1 & 0 & 0 & X_0 \\ 0 & 0 & 0 & 0 \\ 0 & 0 & 0 & 0 \\ X_0^* & 0 & 0 & 0 \end{pmatrix} + \mathcal{O}\left(\frac{g_I^2}{r_{12}^{2(2I+1)}}\right), \quad (3.5)$$

but with

$$X_0 := -2ig_I \frac{Q_1^{I_1} N_{I_1 I_2}(\hat{r}_{12}) Q_2^{I_2}}{r_{12}^{2I+1}} \int_{-\infty}^{\infty} dt w(t) e^{2i\Omega t} . \quad (3.6)$$

The $\mathcal{O}\left(\frac{g_I^2}{r_{12}^{2(2I+1)}}\right)$ in (3.5) can also be obtained analytically, but the form is a little tedious. However, it will be suppressed if g_I is small or r_{ij} is large. We will assume this is the case and consider ρ_{12}^f only up to $\mathcal{O}(g_I)$.

The term X_0 of (3.6) is generally nonzero, yielding entanglement harvesting measured by concurrence. In this work, we choose the Gaussian window function,

$$w_T(t) = \frac{1}{(2\pi)^{1/4}} e^{\frac{-t^2}{4T^2}}, \quad (3.7)$$

such that $\int_{-\infty}^{\infty} |w_T(t)|^2 dt = T$. Then,

$$X_0 = -2(8\pi)^{1/4} ig_I \frac{Q_1^{I_1} N_{I_1 I_2}(\hat{r}_{12}) Q_2^{I_2}}{r_{12}^{2I+1}} T e^{-4\Omega^2 T^2}, \quad (3.8)$$

which is nonzero unless in the limit $\Omega T \rightarrow \infty$ or $r_{12} \rightarrow \infty$. This result can be compared with the one obtained from the direct calculation without using EFT approximation. For simplicity, consider the case of scalar type, i.e., omitting the index I . The $O_{12} \sim Q_1 Q_2$ in (3.4) is replaced by $O_{12} \sim Q_1 Q_2 \langle \Phi(x) \Phi(x') \rangle$. Since $\langle \Phi(x) \Phi(x') \rangle$ for a massless scalar mediator field Φ in flat spacetime is nonvanishing only on the lightcone, it vanishes for a pair of space-like separated x and x' , i.e., the location of UDW detectors. However, when the UDW detectors are held statically by an external force (off-shell), then $\langle \Phi(x) \Phi(x') \rangle \sim 1/|x - x'|$ yielding (3.8).

3.2 Case II: Neglecting direct interaction between UDW detectors

The second case we consider is to assume

$$|Q_{1,2}^I| \ll |Q_B^I|, \quad (3.9)$$

so that the term of $O_{12}^I(t)J_1(t) \otimes J_2(t)$ in (3.2) can be neglected. This setting is similar to the one considering the entanglement harvesting around the warm horizon, such as the ones for a black hole, de Sitter space, or Rindler space [16, 21, 48]. In contrast to the conventional approach, here we first integrate out the mediator field and adopt the EFT approach without directly dealing with the Wightman function of the mediator field. In this case, the evolution operator of (3.2) of a specific type I is reduced to

$$U_{w_T} = \mathcal{T} e^{-ig_I \int_{-\infty}^{\infty} dt w_T(t) \sum_{a=1,2} O_{aB}^I(t) J_a(t)}. \quad (3.10)$$

The condition (3.9) also ensures that the backreaction to ρ_B during the evolution is neglected.

To obtain the reduced state from (3.1) employing the evolution operator (3.10), we assume the initial state ρ_{12}^i of the static UDW detectors to be $|0\rangle_1 \otimes |0\rangle_2$ which is free of any RQI so that the RQI in the final reduced state can be attributed to the extraction from the ambient field. Moreover, we also assume no background value of Q_B^I , i.e., $\langle Q_B^I \rangle = 0$. This is the statement of no-hair theorem if the blackbody is a black hole. Up to $\mathcal{O}\left(\frac{g_I}{r_{ij}^{2(2I+1)}}\right)$, the final reduced state takes the form of X -state [49] as follows:

$$\rho_{12}^f = \begin{pmatrix} 1 - P_1 - P_2 & 0 & 0 & X \\ 0 & P_2 & C & 0 \\ 0 & C^* & P_1 & 0 \\ X^* & 0 & 0 & 0 \end{pmatrix} + \mathcal{O}\left(\frac{g_I^2}{r_{ij}^{4(2I+1)}}\right), \quad (3.11)$$

where

$$P_a := g_I^2 \frac{M_{aI_1} M_{aI_2}}{r_{aB}^{2(2I+1)}} P_T^{I_1 I_2}(\Omega), \quad (3.12)$$

$$C := g_I^2 \frac{M_{1I_1} M_{2I_2}}{r_{1B}^{2I+1} r_{2B}^{2I+1}} P_T^{I_1 I_2}(\Omega), \quad (3.13)$$

$$X := -g_I^2 \frac{M_{1I_1} M_{2I_2}}{r_{1B}^{2I+1} r_{2B}^{2I+1}} X_T^{I_1 I_2}(\Omega), \quad (3.14)$$

with

$$M_{aI_1} := Q_a^I N_{II_1}(\hat{r}_{aB}), \quad (3.15)$$

and

$$P_T^{I_1 I_2}(\Omega) := \int_{-\infty}^{\infty} dt \int_{-\infty}^{\infty} dt' w_T(t) w_T(t') e^{-i\Omega(t-t')} \langle Q_B^{I_1}(t) Q_B^{I_2}(t') \rangle, \quad (3.16)$$

$$X_T^{I_1 I_2}(\Omega) := \int_{-\infty}^{\infty} dt \int_{-\infty}^{\infty} dt' w_T(t) w_T(t') e^{-i\Omega(t+t')} \langle Q_B^{I_1}(t) Q_B^{I_2}(t') \rangle. \quad (3.17)$$

Note that this form of X -state is also obtained in [14–16] by directly dealing with the Wightman function of the mediator field around a warm horizon. Moreover, from (3.12) and (3.13) we have an exact relation

$$C^2 = P_1 P_2, \quad (3.18)$$

which will be helpful when evaluating some of the RQI measures later on.

Adopting the Gaussian window function (3.7) for $w_T(t)$, and using the following fact when performing the change of time variables by $t_{\pm} = t \pm t'$

$$\int_{-\infty}^{\infty} dt \int_{-\infty}^{\infty} dt' w_T(t)w_T(t') e^{-i\Omega(t\pm t')} = \frac{1}{2} \int_{-\infty}^{\infty} dt_- \int_{-\infty}^{\infty} dt_+ w_T\left(\frac{t_-}{\sqrt{2}}\right)w_T\left(\frac{t_+}{\sqrt{2}}\right)e^{-i\Omega t_{\pm}}, \quad (3.19)$$

we can arrive

$$P_T^{I_1 I_2}(\Omega) = (2\pi)^{1/4} T \int_{-\infty}^{\infty} dt_- e^{-i\Omega t_-} w_T\left(\frac{t_-}{\sqrt{2}}\right) \langle Q_B^{I_1}(t_-) Q_B^{I_2}(0) \rangle, \quad (3.20)$$

$$X_T^{I_1 I_2}(\Omega) = (2\pi)^{1/4} T e^{-\Omega^2 T^2} \int_{-\infty}^{\infty} dt_- w_T\left(\frac{t_-}{\sqrt{2}}\right) \langle Q_B^{I_1}(t_-) Q_B^{I_2}(0) \rangle. \quad (3.21)$$

In the above, we have used the fact that $\langle Q_B^{I_1}(t) Q_B^{I_2}(t') \rangle$ is time translational invariant so that $\langle Q_B^{I_1}(t) Q_B^{I_2}(t') \rangle = \langle Q_B^{I_1}(t_-) Q_B^{I_2}(0) \rangle$.

Furthermore, using the convolution theorem, we have

$$\int_{-\infty}^{\infty} dt_- e^{-i\Omega t_-} w_T\left(\frac{t_-}{\sqrt{2}}\right) \langle Q_B^{I_1}(t_-) Q_B^{I_2}(0) \rangle = \sqrt{2} \int_0^{\infty} d\omega \tilde{w}_T[\sqrt{2}(\omega - \Omega)] S^{I_1 I_2}(\omega), \quad (3.22)$$

where the spectral density $S^{I_1 I_2}(\omega)$ is assumed to be bounded below, i.e., it vanishes for $\omega < 0$, and the Fourier transform of $w_T(t)$ is

$$\tilde{w}_T[\omega] = (8\pi)^{1/4} T e^{-\omega^2 T^2}. \quad (3.23)$$

Thus, $\tilde{w}_T[\sqrt{2}(\omega - \Omega)]$ is roughly a window function in frequency domain centered around $\omega = \Omega$ with the window size of $\mathcal{O}(1/T)$. We are in the low-energy regime constrained by (2.8) so that $S^{I_1 I_2}(\omega)$ for the black body is nearly ω -independent as discussed in (2.15), i.e., $S^{I_1 I_2}(\omega) \simeq S^{I_1 I_2}(0)$ if $\beta\omega \ll 1$. Thus, combining all the above, $P_T^{I_1 I_2}$ and $X_T^{I_1 I_2}$ can be approximated to be

$$P_T^{I_1 I_2}(\Omega) \simeq \pi T [1 + \text{erf}(\sqrt{2}\Omega T)] S^{I_1 I_2}(0), \quad (3.24)$$

$$X_T^{I_1 I_2}(\Omega) \simeq \pi T e^{-2\Omega^2 T^2} S^{I_1 I_2}(0). \quad (3.25)$$

This implies that

$$X_T^{I_1 I_2}(\Omega) \leq P_T^{I_1 I_2}(\Omega), \quad (3.26)$$

Thus, also by (3.12) and (3.14) it yields

$$|X|^2 \leq P_1 P_2. \quad (3.27)$$

We shall remark that the reduced final state of (3.11) is evaluated up to $\mathcal{O}(g_I)$ instead of $\mathcal{O}(g_I^2)$. Formally, P_a , C and X are $\mathcal{O}(g_I^2)$ as shown in (3.12) to (3.14). However, they are in fact $\mathcal{O}(g_I)$ because $P_T^{I_1 I_2}$ and $X_T^{I_1 I_2}$ contain a factor of $1/g_I$ inherited from $B^{I_1 I_2}$ of (2.16), which is the low-energy expression of $S^{I_1 I_2}(\omega)$, i.e., (2.15).

3.3 Case III: Including all direct interactions

Finally, the last case is to consider the full evolution operator (3.2) of a particular I -type without truncation as adopted in the first and second examples. The reduced final state takes the form of the full X -state as follows:

$$\rho_{12}^f = \begin{pmatrix} 1 - P_1 - P_2 - P_{12} & 0 & 0 & X + X_0 \\ 0 & P_2 & C & 0 \\ 0 & C^* & P_1 & 0 \\ X^* + X_0^* & 0 & 0 & P_{12} \end{pmatrix} + \mathcal{O}\left(\frac{g_I^3}{r_{ij}^{4(2I+1)}}\right), \quad (3.28)$$

where

$$P_{12} = X_0 X_0^*, \quad (3.29)$$

and the other variables are defined earlier. Note that P_{12} is $\mathcal{O}(g_I^2)$ since X_0 is $\mathcal{O}(g_I)$. However, to go beyond $\mathcal{O}(g_I)$ result, we also need to include higher order terms when expanding the evolution operator U_{w_T} of (3.2) to yield complete ρ_{12}^f up to $\mathcal{O}(g_I^2)$. In this paper, we will restrict to $\mathcal{O}(g_I)$ result and neglect P_{12} from now on.

We now consider the dependence of the matrix elements in (3.28) on the scales such as T , \bar{r}_i , r_{ij} and Ω . Note that these scales should satisfy (2.8) for low-energy EFT to be valid. Dimensional-wise,

$$|Q_a^I| = q_a \bar{r}_a^I, \quad a = 1, 2, \quad (3.30)$$

with the dimensionless q_a to denote the strength of the corresponding multiple moments. Along with the scaling relation of $B^{I_1 I_2}$ of (2.16), the scale dependence can be expressed as

$$P_a \sim g_I q_a^2 \left(\frac{\bar{r}_a}{r_{aB}}\right)^{2I} \left(\frac{\bar{r}_B}{r_{aB}}\right)^{2I+1} \frac{T}{r_{aB}}, \quad X_0 \sim g_I q_1 q_2 \left(\frac{\bar{r}_1 \bar{r}_2}{r_{12}^2}\right)^I \frac{T}{r_{12}} e^{-4\Omega^2 T^2}, \quad (3.31)$$

$$C \sim g_I q_1 q_2 \left(\frac{\bar{r}_1 \bar{r}_2}{r_{1B} r_{2B}}\right)^I \left(\frac{\bar{r}_B^2}{r_{1B} r_{2B}}\right)^I \left(\frac{\bar{r}_B T}{r_{1B} r_{2B}}\right), \quad X \sim C e^{-2\Omega^2 T^2}, \quad P_{12} = |X_0|^2. \quad (3.32)$$

Note that P_{12} is one order higher in g than the other elements. Thus, we can neglect it if we restrict to $g_I \ll 1$ by considering just leading order EFT. Based on the above scaling relation, we have

$$\frac{X_0}{X} \sim \left(\frac{r_{1B} r_{2B}}{r_{12}^2}\right)^I \left(\frac{r_{1B} r_{2B}}{\bar{r}_B^2}\right)^I \left(\frac{r_{1B} r_{2B}}{r_{12} \bar{r}_B}\right) e^{-2\Omega^2 T^2} \sim \left(\frac{r_{aB}}{\bar{r}_B}\right)^{2I+1} e^{-2\Omega^2 T^2}. \quad (3.33)$$

In arriving last expression, we have assumed $r_{1B} \simeq r_{2B} \simeq r_{12}$. To ensure (3.10) and (3.11), we have assumed (3.9). With the help of (3.33) and the conditions (2.8) for EFT to hold, we can now turn (3.9) into a more precise one by requiring $X_0 \ll X$. From (2.8), one should require $r_{aB} \gg \bar{r}_B$, so that $X_0 \ll X$ holds only if \bar{r}_B or ΩT is large enough, i.e.,

$$X_0 \ll X \implies \bar{r}_B^{2I+1} \gg r_{aB}^{2I+1} e^{-2\Omega^2 T^2} \quad \text{or} \quad 2(\Omega T)^2 \gg (2I+1) \ln\left(\frac{r_{aB}}{\bar{r}_B}\right). \quad (3.34)$$

This, however, can be achieved without any problem.

3.4 Features of reduced final states and RQI measures

The reduced final state ρ_{12}^f of the bipartite UDW detectors for all three scenarios are in the special cases of X -states characterized by parameters X , X_0 , P_1 , and P_2 . The key features of ρ_{12}^f up to $\mathcal{O}(g)$ can be summarized as follows:

(i) Case I contains only nonzero $(\rho_{12}^f)_{14} = (\rho_{12}^f)_{41} = X_0$.

(ii) Case II is constrained by $|C|^2 = P_1 P_2$.

(iii) Adding ρ_{12}^f 's of Case I and II to get the one of Case III, for which $|C|^2 = P_1 P_2$ remains.

One way to characterize X -states in the form of (3.28) is by its eigenvalues $\{\lambda_{0,1,\pm}\}$ (up to $\mathcal{O}(g)$):

$$\lambda_{0,1,\pm} = 0, \quad 1 - P_1 - P_2, \quad \frac{1}{2} \left(P_1 + P_2 \pm \sqrt{(P_1 - P_2)^2 + 4|C|^2} \right). \quad (3.35)$$

They do not depend on the value of X or X_0 . As a result, Case II and III have the same eigenvalues. Moreover, due to the constraint $|C|^2 = P_1 P_2$, the eigenvalues of (3.35) are further simplified as

$$\lambda = 0, \quad 1 - P_1 - P_2, \quad P_1 + P_2, \quad 0. \quad (3.36)$$

Thus, ρ_{12}^f considered in this paper is at most rank two.

Below, we will consider three RQI measures:

1. Concurrence \mathcal{C} to characterize the entanglement harvesting [50] from the ambient quantum field. For X -states considered, concurrence $\mathcal{C} \sim \max\{0, |X| - \sqrt{P_1 P_2}\}$ is independent of C [15, 16]. Immediately, we see that \mathcal{C} is non-zero for Case I, but vanishes for Case II due to (3.27).
2. Quantum discord \mathcal{D} characterizing non-classical quantum correlation [36, 37]. For the X -states considered, \mathcal{D} is independent of $(\rho_{12}^f)_{14} = (\rho_{12}^f)_{41}$, i.e., X and X_0 . This leads us to conclude that there is no pure quantum correlation for Case I, and the quantum discord is the same for Case II and III up to $\mathcal{O}(g)$.
3. Bipartite nonlocality bound S_ρ for CHSH-type experiment [38–40] characterizes the nature of correlations. It depends on all the parameters in ρ_{12}^f of X -states considered. We will see that the EFT action (2.2) is consistent with the RQI locality.

From the above discussion, we observe that RQI encoded in \mathcal{C} and \mathcal{D} are complementary.

In the following sections, we will examine these RQI measures for the reduced final states across all three cases in greater detail. For simplicity, when presenting the numerical plots of the RQI measures, we will consider only the scalar-type environmental field, i.e., the tensor index I will be absent. Also, we choose $g_0 = 0.01$ to ensure the validity of perturbative results, along with fixing $\bar{r}_B = \bar{r}_1 = \bar{r}_2 = 1$, $q_1 = q_2 = 1$ for convenience. Furthermore, we fix a tiny energy gap $\Omega = 0.001$, so that T can be large enough to satisfy the condition (2.8) for the validity of EFT. Thus, we will only focus on the dependence of the RQI measures on interaction time T , the inter-distances r_{12} and r_{1B} . Furthermore, we also confirm that the purity of all cases remains non-negative and bounded below one, ensuring physically valid reduced final states.

4 Entanglement Harvesting

The entanglement harvesting by the UDW detectors can be quantified by evaluating the concurrence [50]. For (3.11) of the X -state, it is given by [15, 16]

$$\mathcal{C}(\rho_{12}^f) = 2 \max\{0, |X| - \sqrt{P_1 P_2}\}. \quad (4.1)$$

The concurrence is an entanglement monotone and is zero for a separable pure state. Since we start with the pure separable state $\rho_{12}^i = |0\rangle_1 \otimes |0\rangle_2$ of vanishing entanglement, any nonzero value of concurrence (4.1) quantifies the entanglement harvested by the pair of UDW detectors from the environmental field's quantum state.

4.1 Case I

Consider the entanglement harvesting of the first case for which the black hole is absent, and ρ_{12}^f is given by (3.5) and (3.6), which is in a particular form of X -state given in (3.11) with $P_1 = P_2 = C = 0$ and $X = X_0$. Then from (4.1), we see that there is a nonzero concurrence

$$\mathcal{C}(\rho_{12}^f) = 2|X_0| = 4(8\pi)^{1/4} g_0 \frac{Q_1 N(\hat{r}_{12}) Q_2}{r_{12}} T e^{-4\Omega^2 T^2}, \quad \text{for } \rho_{12}^f = (3.5). \quad (4.2)$$

This implies the pair of UDW detectors can harvest entanglement via the mutual Coulombic interaction. The amount of the harvested entanglement decays with the interaction time T exponentially and the separation r_{12} in the power-law. Some typical patterns of (4.2) are shown in fig. 2. Note that the entanglement harvesting reaches a maximum around the interaction time to match the given energy gap, i.e., $\Omega T \sim \mathcal{O}(1)$. This is because the transport of the RQI is facilitated by the process of conserving energy.

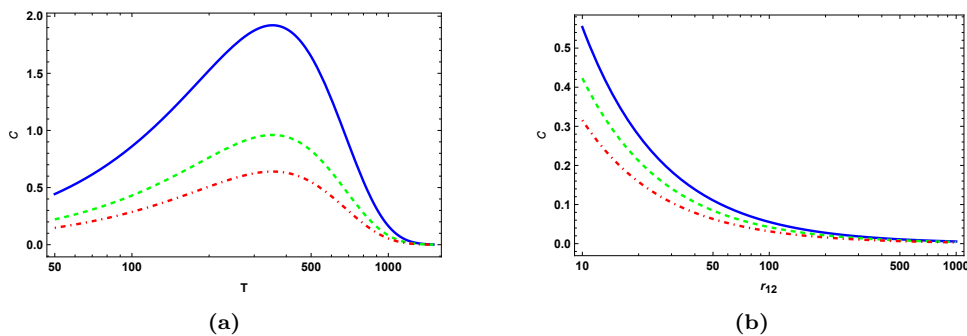


Figure 2: Concurrence \mathcal{C} for ρ_{12}^f of (3.5): (a) \mathcal{C} vs T for various r_{12} : $r_{12} = 10$ (solid-blue), $r_{12} = 20$ (green-dashed) and $r_{12} = 30$ (red-dot-dashed). (b) \mathcal{C} vs r_{12} for various T : $T = 800$ (solid-blue), $T = 850$ (green-dashed) and $T = 900$ (red-dot-dashed). In this figure and the other ones shown later on, we fix $g_0 = 0.01$, $\Omega = 0.001$ and $\bar{r}_B = \bar{r}_1 = \bar{r}_2 = 1$, $q_1 = q_2 = 1$.

As the mediator field effect is only taken out at the tree level to yield Coulombic interaction, the mediator field shall behave as a classical environment. Thus, our result is counter-intuitive to the expectation of no quantum information in the classical environment. This seeming contradiction could be due to the instantaneous nature of the Coulomb-like force, which couples the spins of off-shell static UDW detectors remotely and instantaneously.

4.2 Case II

We now consider the entanglement harvesting for the second case, i.e., having the black hole but neglecting the direct interaction between UDW detectors. As mentioned before, due to the relation (3.27), i.e., $|X|^2 \leq P_1 P_2$, in the low energy regime $\beta\omega \ll 1$, we can conclude

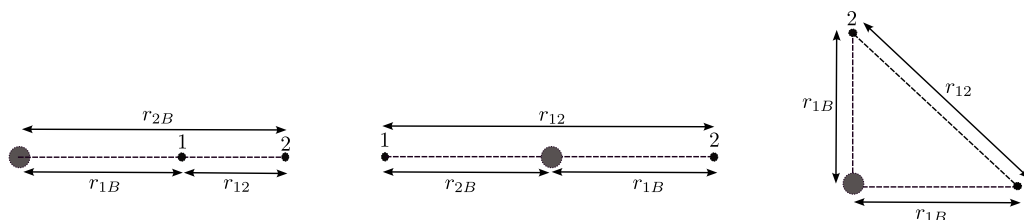
$$\mathcal{C}(\rho_{12}^f) = 0 \quad \text{for} \quad \rho_{12}^f = (3.11). \quad (4.3)$$

We can go to $\mathcal{O}(\beta\omega)$ of (2.15), and the above result will not change. This result implies that one cannot harvest entanglement from a quantum blackbody such as a quantum black hole in the low-energy regime. Our result differs from the one by using master field theory, which yields non-vanishing entanglement harvesting from the ambient field thermalized by the event horizon [16, 21, 48]. We may conclude that the entanglement harvesting around the event horizons may come from the high-energy regime. However, as we will see in the next case, we can recover these patterns of entanglement harvesting by also including the mutual Coulombic interaction among UDW detectors. This implies that all the EFT interactions in the same order of PN expansion are relevant to recovering the total result of the master field theory.

4.3 Case III

This subsection considers the entanglement harvesting for the third case, where all the interactions of the EFT are taken into account. The harvested entanglement is quantified by concurrence, which is given as

$$\mathcal{C}(\rho_{12}^f) = 2 \max\{0, |X + X_0| - \sqrt{P_1 P_2}\} \quad \text{for} \quad \rho_{12}^f = (3.28). \quad (4.4)$$



(a) Line-up configuration with a black hole at leftmost.

(b) Line-up configuration with a black hole in the middle.

(c) Configuration with a black hole at right-angle vertex.

Figure 3: Three configurations of UDW detectors (small black dots) relative to the black hole (big black dot).

To facilitate comparison with the results of [16], obtained using the conventional approach based on master theory, we examine three configurations of UDW detector placement relative to the black hole. In configuration a, illustrated in fig. 3a, both UDW detectors are positioned along a straight line on the right side of the black hole. The configuration b, depicted in fig. 3b, places the black hole between the two UDW detectors. Finally, in configuration c, shown in fig. 3c, the detectors are arranged so that they, together with the black hole, form a right triangle. We will also consider some of these configurations when evaluating the quantum discord (section 5) and nonlocality bound (section 6).

4.3.1 Configuration a

The configuration of fig. 3a is specified by two parameters: the distance r_{1B} between the black hole and the nearest UDW detector to the black hole, and r_{12} the inter-distance between two UDW detectors. We will then present the concurrence as a function of T , r_{1B} , and r_{12} with all other parameters fixed to the values mentioned before.

In fig. 4, we present the concurrence for this configuration of ρ_{12}^f of (3.28) as a function of T in fig. 4a, of r_{1B} in fig. 4b and of r_{12} in fig. 4c by fixing the other parameters. The behavior of concurrence in fig. 4a resembles the one in fig. 2a with a maximum around $\Omega T \sim \mathcal{O}(1)$, but with a subtle difference: there exists a “sudden death” at large enough T in fig. 4a but not in fig. 2a. This indicates that the existence of the event horizon will change the patterns of entanglement harvesting qualitatively.

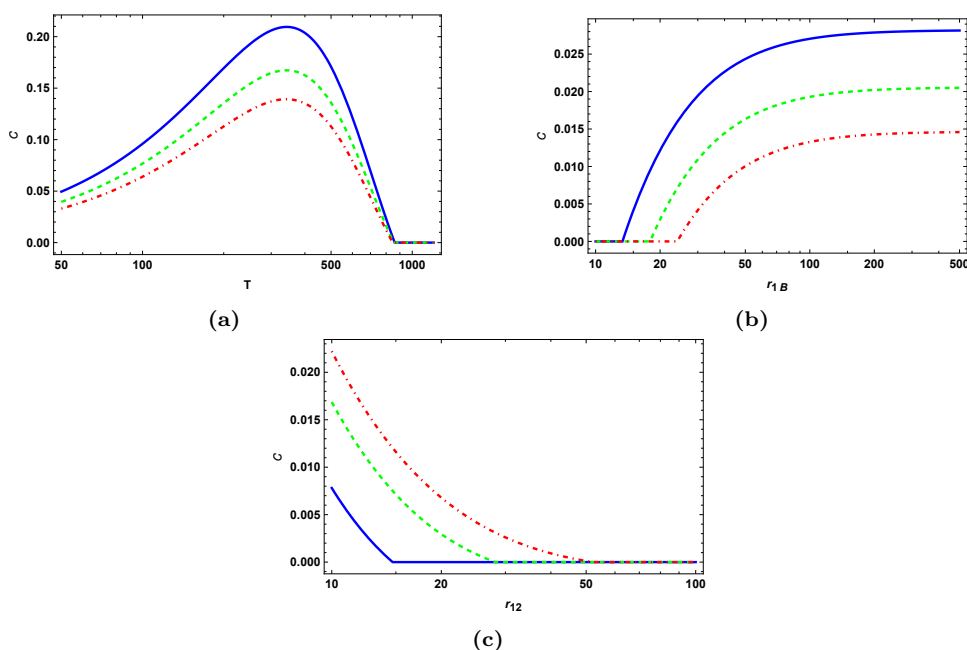


Figure 4: Concurrence C of configuration fig. 3a for ρ_{12}^f of (3.28): (a) C vs T for $r_{1B} = 10$ and various r_{12} : $r_{12} = 20$ (solid-blue), $r_{12} = 25$ (green-dashed) and $r_{12} = 30$ (red-dot-dashed). (b) C vs r_{1B} for $r_{12} = 25$, and various T : $T = 900$ (solid-blue), $T = 950$ (green-dashed) and $T = 1000$ (red-dot-dashed). (c) C vs r_{12} for $T = 100$, and various r_{1B} : $r_{1B} = 20$ (solid-blue), $r_{1B} = 25$ (green-dashed) and $r_{1B} = 30$ (red-dot-dashed).

The “sudden death” of the concurrence also occurs when r_{1B} falls below some critical values as shown in fig. 4b or when r_{12} grows beyond some critical values as shown in fig. 4c. Note also that the concurrence saturates to a constant value when the detectors are far from the black hole. All of the patterns of entanglement harvesting, as shown in fig. 4b and fig. 4c are qualitatively the same as the ones observed in [16] by evaluating the entanglement harvesting with the master theory, and there, the region of vanishing concurrence was coined as “entanglement shadow”. Notably, the size of “entanglement shadow” increases with the detector’s energy gap. The agreement on the patterns of fig. 4b obtained by both EFT and its master theory can be seen as a consistency check of the EFT approach. However, the reduced final states of UDW detectors can be evaluated more transparently in the EFT than in the master theory without dealing with

the thermal correlators of the ambient field in the black hole background.

The existence of the “entanglement shadow” is closely related to the decoherence of a quantum object near a black hole [1, 9–11]. The decoherence becomes stronger as the quantum object, e.g., the qubit UDW detector moves closer to the black hole or the interaction time increases. This is because the effect of thermal noises due to Hawking radiation becomes larger in such cases. Thus, when one of the UDW detectors enters the “entanglement shadow”, the decoherence becomes strong, resulting in sudden death, as shown in fig. 4b. Similarly, if the pair of UDW detectors are too far separated to be coherently correlated for entanglement harvesting, then the “sudden death” occurs, as shown in fig. 4c.

4.3.2 Configuration b

For simplicity, when considering the configuration of fig. 3b, we set $r_{1B} = r_{2B}$ so that $r_{12} = 2r_{1B}$. Thus, we will consider the concurrence as a function of T and $r_{1B} = \frac{r_{12}}{2}$ by fixing all the other parameters to the values mentioned before. We then plot \mathcal{C} vs T for a given r_{1B} in fig. 5a, and \mathcal{C} vs r_{1B} for a given T in fig. 5b. The pattern shown in fig. 5a is almost the same as in fig. 4a. As in fig. 4b, there also exists “entanglement shadow” in fig. 5b. By comparison, we find that the size of the “entanglement shadow” for a given T is larger in fig. 5b than in fig. 4b. This is understandable because, in the current configuration, both UDW detectors move together toward the back hole so that the thermal noise effect of causing decoherence is more severe in inhibiting entanglement harvesting than in the configuration of fig. 3a. Moreover, the concurrence at large r_{1B} is no longer saturated to a constant value but decays to zero simply because now $r_{12} = 2r_{1B}$. Thus, the large r_{12} behavior of \mathcal{C} is similar to the one in fig. 2b.

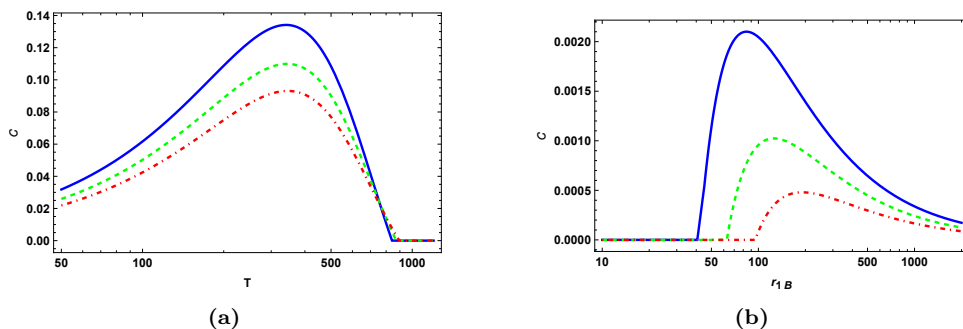


Figure 5: Concurrence \mathcal{C} of configuration fig. 3b for ρ_{12}^f of (3.28): (a) \mathcal{C} vs T for various r_{1B} : $r_{1B} = 20$ (solid-blue), $r_{1B} = 25$ (green-dashed) and $r_{2B} = 30$ (red-dot-dashed). (b) \mathcal{C} vs r_{1B} for various T : $T = 900$ (solid-blue), $T = 950$ (green-dashed) and $T = 1000$ (red-dot-dashed).

4.3.3 Configuration c

For a given set of (r_{1B}, r_{2B}) , $r_{12} = r_{1B} + r_{2B}$ for configuration of fig. 3b, and $r_{12} = \sqrt{(r_{1B}^2) + (r_{2B}^2)}$ for configuration of fig. 3c. Thus, the difference between the configurations b and c will only cause a difference in X_0 . If we further set $r_{1B} = r_{2B}$ as considered for configuration b, we expect their results to be qualitatively similar. This is the case when comparing fig. 5 and fig. 6 which consists of \mathcal{C} vs T for a given r_{1B} in fig. 6a, and \mathcal{C} vs r_{1B} for a given T in fig. 6b.

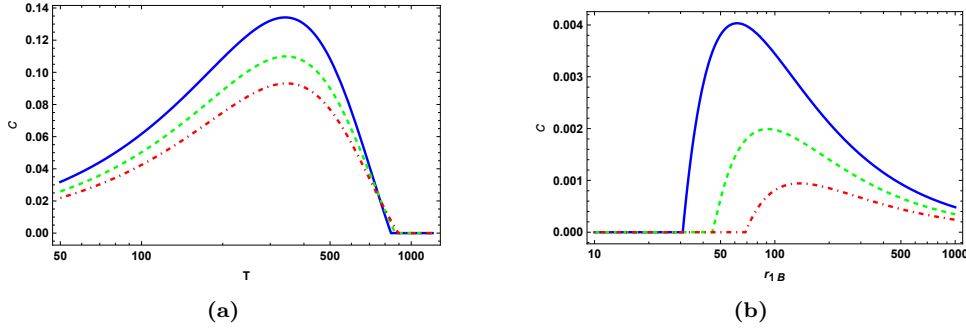


Figure 6: Concurrence C of configuration fig. 3c for ρ_{12}^f of (3.28): (a) C vs T for various r_{1B} : $r_{1B} = 20$ (solid-blue), $r_{1B} = 25$ (green-dashed) and $r_{1B} = 30$ (red-dot-dashed). (b) C vs r_{1B} for various T : $T = 900$ (solid-blue), $T = 950$ (green-dashed) and $T = 1000$ (red-dot-dashed).

Thus, we will not consider the configuration of fig. 3c when discussing the quantum discord and nonlocality bound in the following sections.

5 Quantum Discord

In this section, we discuss the characterization of the quantum correlation of the UDW detectors by computing quantum discord, which excludes the classical correlation from the quantum mutual information. Thus, we can use the quantum discord to quantify the quantumness of a quantum state from the point of view of RQI.

For a bipartite system composed of A and B , the quantum discord is defined by [36, 37]

$$\mathcal{D}(\rho_{AB}) := \min_{\{B_k\}} \sum_k p_k S(A||B_k) - S(A||B) \geq 0, \quad (5.1)$$

where the relative entropy $S(A||B) := S(AB) - S(B)$ with the von Neumann entropy $S(A) := -\text{Tr}_A \rho_A \ln \rho_A$, $\{B_k\}$ is a projective measurement basis for performing measurements on subsystem B , and $p_k := \text{Tr}_B(B_k \rho_{AB})$. The quantum discord vanishes when ρ_{AB} is a pointer state, i.e., $\rho_{AB} = \sum_k B_k \rho_{AB} B_k$. Usually, evaluating quantum discord is tedious for general X -state to carry out the minimization over possible measurement bases [51–53]. However, in [21], we find that the quantum discord for the X -state (3.11) up to $\mathcal{O}(g)$ is independent of the measurement basis, and the result is

$$\begin{aligned} \mathcal{D}(\rho_{12}^f) &= \frac{1}{2 \ln 2} \left[(P_1 + P_2) \ln(P_1 P_2 - C^2) - 2P_1 \ln P_1 - 2P_2 \ln P_2 \right. \\ &\quad \left. + \sqrt{(P_1 - P_2)^2 + 4C^2} \ln \frac{P_1 + P_2 + \sqrt{(P_1 - P_2)^2 + 4C^2}}{P_1 + P_2 - \sqrt{(P_1 - P_2)^2 + 4C^2}} \right]. \end{aligned} \quad (5.2)$$

Note that when $C^2 = P_1 P_2$, (5.2) is simplified to

$$\mathcal{D}(\rho_{12}^f) = \frac{1}{2 \ln 2} \left[-P_1 \ln P_1 - P_2 \ln P_2 + (P_1 + P_2) \ln(P_1 + P_2) \right]. \quad (5.3)$$

On the other hand, if $P_1 = P_2 := P$, (5.2) can be reduced to

$$\mathcal{D}(\rho_{12}^f) = \frac{1}{\ln 2} \left[(P + |C|) \ln(P + |C|) + (P - |C|) \ln(P - |C|) - 2P \ln P \right], \quad (5.4)$$

which can be further reduced to $\mathcal{D}(\rho_{12}^f) = 2P$ if additionally $C = P$.

5.1 Case I

As mentioned earlier, there is no quantum discord when there is no direct interaction between the black hole and the UDW detectors as $P_1 = P_2 = C = 0$. This suggests that the Coulombic force cannot create a pure quantum correlation between two UDW qubits but can provide nonzero entanglement eq. (4.2).

5.2 Case II and III

As discussed before, for the X -states up to $\mathcal{O}(g)$, the quantum discord is independent of $(\rho_{12}^f)_{14} = (\rho_{12}^f)_{41}$, i.e., X or X_0 , thus it will be the same for Case II and Case III even though only the latter can have nonzero concurrence. Furthermore, using (3.18), we notice that the quantum discord for both cases is given by (5.3).

In the following, we present the corresponding quantum discord for the configurations of figs. 3a and 3b, respectively.

5.2.1 Configuration a

The results of quantum discord for the configuration of fig. 3a obtained by (5.3) are presented in fig. 7 with \mathcal{D} as a function of T in fig. 7a, of r_{12} in fig. 7b, and of r_{1B} in fig. 7c by fixing rest of the parameters.

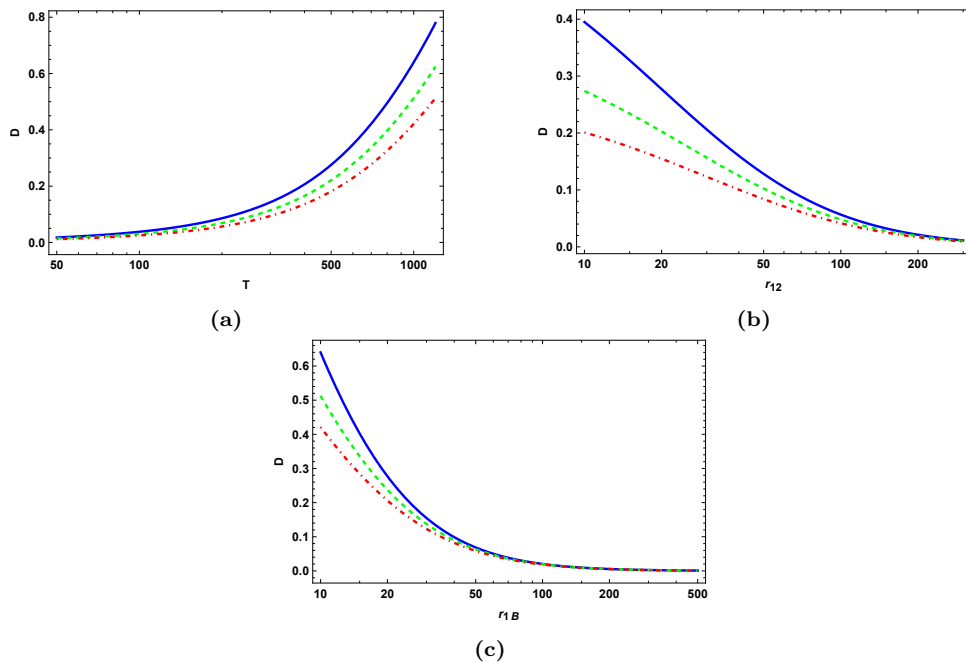


Figure 7: Quantum discord \mathcal{D} of configuration fig. 3a for ρ_{12}^f of (3.28): (a) \mathcal{D} vs T for $r_{1B} = 10$ and various r_{12} : $r_{12} = 20$ (solid-blue), $r_{12} = 25$ (green-dashed) and $r_{12} = 30$ (red-dot-dashed). (b) \mathcal{D} vs r_{1B} for $T = 1000$, and various r_{12} : $r_{12} = 20$ (solid-blue), $r_{12} = 25$ (green-dashed) and $r_{12} = 30$ (red-dot-dashed). (c) \mathcal{D} vs r_{12} for $T = 100$, and various r_{1B} : $r_{1B} = 20$ (solid-blue), $r_{1B} = 25$ (green-dashed) and $r_{1B} = 30$ (red-dot-dashed).

We observe that the results for the quantum discord are consistent with the usual expectations. Specifically, the pure quantum correlation grows monotonically as the interaction time increases and monotonically diminishes as the inter-distance between UDW detectors increases. Unlike

the bump behavior of concurrence shown in fig. 5b, quantum discord decreases monotonically as the UDW detectors with a fixed separation move away from the black hole. Besides, the key feature distinguishing the concurrence and quantum discord is the absence of “sudden death” behavior for the latter. This implies that the UDW detectors are quantum correlated with the black hole, and the thermal noise of Hawking radiation will not affect the pure quantum correlations but may affect the classical one. Furthermore, from fig. 7b and fig. 7c, we find that discord decays more rapidly with r_{1B} than with r_{12} .

5.2.2 Configuration b

The results of quantum discord for the configuration of fig. 3b with $r_{1B} = r_{2B} = r_{12}/2$ are presented in fig. 8: \mathcal{D} vs T for various r_{1B} in fig. 8a, and \mathcal{D} vs r_{1B} for various T in fig. 8b. The patterns found here are similar to the ones of fig. 7, and bear analogous implications.

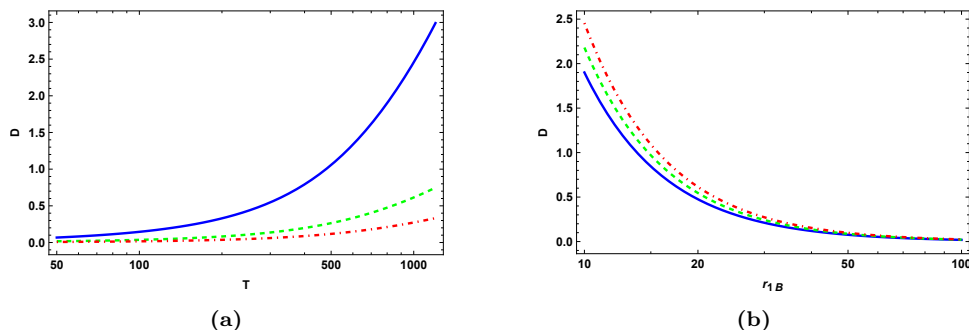


Figure 8: Quantum discord \mathcal{D} of configuration fig. 3b for ρ_{12}^f of (3.28): (a) \mathcal{D} vs T for various r_{1B} : $r_{1B} = 20$ (solid-blue), $r_{1B} = 25$ (green-dashed) and $r_{1B} = 30$ (red-dot-dashed). (b) \mathcal{D} vs r_{1B} for various T : $T = 800$ (solid-blue), $T = 900$ (green-dashed) and $T = 1000$ (red-dot-dashed).

6 Nonlocality Bound

The EPR paper [54] raised the issue of the nonlocal nature of the quantum entangled states, now recognized as the quantum resource [40, 55] to achieve nontrivial tasks such as quantum teleportation or dense coding [56, 57]. In a broad context, the nonlocality is examined by Bell-type experiments, considering the correlations of measurement outcomes in a bipartite communication channel and devising algebraic inequalities on the combination of the outcome correlation to characterize the nonlocal resource in the communication channel. If there is no nonlocal resource, then the joint probability of the bipartite measurement outcomes take a form admitted by the local hidden variable model (LHVM)

$$p(ab|xy) = \int_{\Lambda} d\lambda q(\lambda) p(a|x, \lambda) p(b|y, \lambda), \quad (6.1)$$

where x and a are respectively Alice’s measurement choice and outcome, and y and b are Bob’s ones, and $q(\lambda)$ is the probability distribution of local hidden variable λ . On the other hand, in quantum mechanics, the joint probability is constructed by

$$p(ab|xy) = \text{tr}(\rho_{AB} M_{a|x} M_{b|y}), \quad (6.2)$$

where $\{M_{a|x}\}$ are the positive operator-valued measure (POVM). Then, there exist some non-locality measures characterized by the following kinds of inequalities [39]

$$\sum_{\{abxy\}} s_{abxy}^k p(ab|xy) \leq S_k. \quad (6.3)$$

Many such inequalities labeled by k may exist. If one of the above inequalities is violated, nonlocal resources will exist in the communication channel.

For our purpose, we will only consider bipartite communication tasks with two-level systems, i.e., $a, b, x, y = \{-1, +1\}$. In such case, the inequality characterizing the nonlocality is the Clauser-Horne-Shimony-Holt (CHSH) inequality

$$S := \langle a_{-1}b_{-1} \rangle + \langle a_{-1}b_{+1} \rangle + \langle a_{+1}b_{-1} \rangle - \langle a_{+1}b_{+1} \rangle \leq 2, \quad (6.4)$$

with $\langle a_x b_y \rangle = \sum_{\{ab\}} ab p(ab|xy)$. Thus, the CHSH nonlocality bound is $S_{k=\text{CHSH}} = 2$. One can also extend the above inequality study from nonlocality to no-signaling [39, 58–60], i.e., with the no-signaling conditions: $p(a|x) = p(a|xy) := \sum_{\{b\}} p(ab|xy)$ and $p(b|y) = p(b|xy) := \sum_{\{a\}} p(ab|xy)$. The no-signaling inequality for the bipartite qubits' *quantum* communication turns out to be the same as (6.4) but replacing $S_{\text{CHSH}} = 2$ with Tsirelson bound $S_{\text{Tsirelson}} = 2\sqrt{2}$.

In this paper, we will adopt the reduced final state ρ_{12}^f of UDW qubits as the communication channel for CHSH inequality, then examine its (non)-locality. In this case, if a quantum state is separable, i.e., $\rho_{AB} = \sum_{\lambda} p_{\lambda} \rho_A^{\lambda} \otimes \rho_B^{\lambda}$, its corresponding $p(ab|xy)$ can be put into the form of (6.1), thus it is local. By the example considered in the EPR paper, one may try to conclude that all the entangled quantum states are nonlocal. In [61–63] it has been proved that all the entangled pure states are nonlocal. However, this is not the case for entangled mixed states, i.e., there are local entangled mixed states such as some of the Werner states [64]. For a quantum state ρ of bipartite qubits, the quantity S in CHSH inequality (6.4), denoting it by S_{ρ} since it is evaluated for a quantum state, is given by [38]

$$S_{\rho} = 2\sqrt{t_{11}^2 + t_{22}^2}, \quad (6.5)$$

where t_{11}^2 and t_{22}^2 are the two largest eigenvalues of the matrix $T_{\rho} T_{\rho}^T$ with the 3×3 matrix $(T_{\rho})_{ij} := \text{tr}[\rho(\sigma_i \otimes \sigma_j)]$ for $i, j = 1, 2, 3$. If $S_{\rho} > S_{\text{CHSH}} = 2$, then the state ρ can be utilized as a nonlocal quantum resource. Unlike concurrence or negativity, S_{ρ} is not an entanglement measure as it is not a monotone under LOCC [65]. Thus, it is possible to have local entangled mixed states, such as will be seen for the ρ_{12}^f considered in this paper. Below, we will evaluate S_{ρ} up to $\mathcal{O}(g)$ to be consistent with the perturbation theory and show its behaviors for Cases I, II, and III.

6.1 Case I

For this case, we find that $S_{\rho} = S_{\text{CHSH}} = 2$, indicating that the CHSH inequality is saturated but not violated for any values of T and r_{12} . This implies that the reduced final state ρ_{12}^f (3.5)

obtained from evolution by Coulombic interaction is entangled but does not violate the CHSH inequality. This local nature of the correlations in the Bell-type experiments is in sharp contrast to the inherently nonlocal/acausal nature of Coulombic forces in a field-theoretic context. This observation suggests that the meaning of locality is contextual, which we will further elaborate in section 7.

6.2 Case II

We now examine the nonlocality bound for Case II with a black hole but not the mutual Coulombic interaction between UDW detectors. We will only consider the configurations of figs. 3a and 3b.

6.2.1 Configuration a

In fig. 9a, we plot S_ρ as a function of T , where we see a monotonic decreasing behavior of S_ρ . The nonlocality bound is not violated for any value of T . Furthermore, we present S_ρ in figs. 9b and 9c with r_{12} and r_{1B} respectively, where we notice S_ρ increases monotonically as r_{12} and r_{1B} grows. Again, the nonlocality bound is not violated for any value of r_{12} and r_{1B} . As S_ρ is not a monotone measure under LOCC, it is unclear if these monotonic behaviors can be interpreted as the degrees of nonlocality of the underlying quantum state. Despite that, these patterns are some physical characteristics of these quantum states.

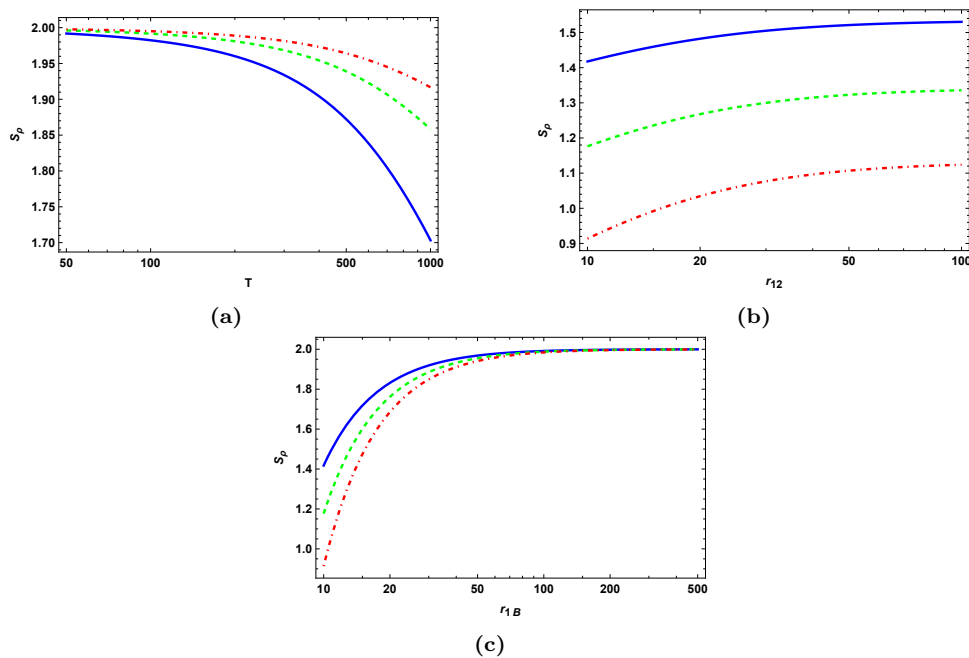


Figure 9: Quantum nonlocality S_ρ for ρ_{12}^f of (3.11): (a) S_ρ vs T for $r_{12} = 20$ and various r_{1B} : $r_{1B} = 50$ (solid-blue), $r_{1B} = 75$ (green-dashed) and $r_{1B} = 100$ (red-dot-dashed). (b) S_ρ vs r_{12} for $r_{1B} = 10$ and various T : $T = 150$ (solid-blue), $T = 200$ (green-dashed) and $T = 250$ (red-dot-dashed). (c) S_ρ vs r_{1B} for $r_{12} = 10$ and various T : $T = 150$ (solid-blue), $T = 200$ (green-dashed) and $T = 250$ (red-dot-dashed).

6.2.2 Configuration b

We present S_ρ as a function of T and r_{1B} in figs. 10a and 10b respectively. The patterns shown here are qualitatively the same as in figs. 9a and 9c. In particular, the CHSH nonlocality bound is not violated for all the parameter ranges considered. This implies that the quantum locality of Case II is configuration-independent.

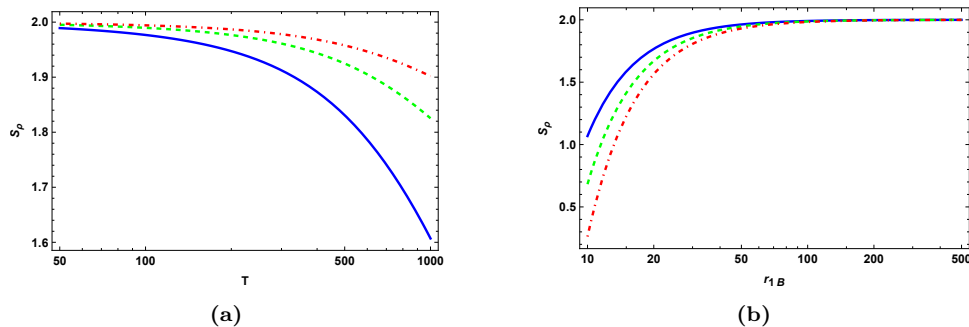


Figure 10: Quantum nonlocality S_ρ for ρ_{12}^f of (3.11): (a) S_ρ vs T for various r_{1B} : $r_{1B} = 50$ (solid-blue), $r_{1B} = 75$ (green-dashed) and $r_{1B} = 100$ (red-dot-dashed). (b) S_ρ vs r_{1B} for various T : $T = 150$ (solid-blue), $T = 200$ (green-dashed) and $T = 250$ (red-dot-dashed).

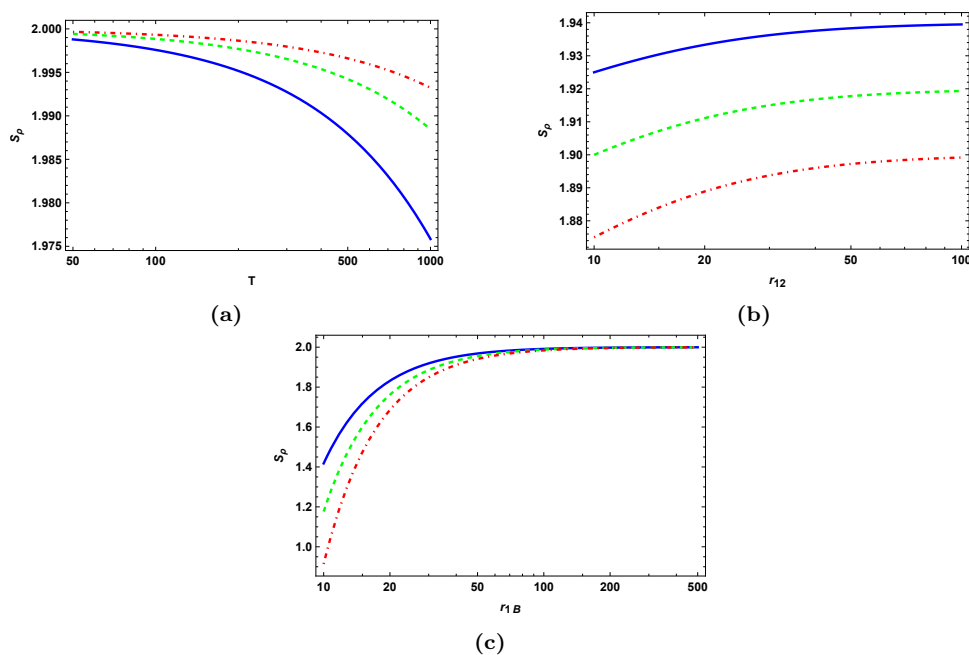


Figure 11: Quantum nonlocality S_ρ for ρ_{12}^f of (3.28): (a) S_ρ vs T for $r_{12} = 20$ and various r_{1B} : $r_{1B} = 50$ (solid-blue), $r_{1B} = 75$ (green-dashed) and $r_{1B} = 100$ (red-dot-dashed). (b) S_ρ vs r_{12} for $r_{1B} = 10$ and various T : $T = 150$ (solid-blue), $T = 200$ (green-dashed) and $T = 250$ (red-dot-dashed). (c) S_ρ vs r_{1B} for $r_{12} = 10$ and various T : $T = 150$ (solid-blue), $T = 200$ (green-dashed) and $T = 250$ (red-dot-dashed).

6.3 Case III

In this subsection, we consider the case when all the interactions of the EFT are considered. Again, S_ρ of the configurations of figs. 3a and 3b will be presented.

6.3.1 Configuration a

We first plot S_ρ as a function of T in fig. 11a where it exhibits a monotonic decreasing behavior. Furthermore, in figs. 11b and 11c we plot S_ρ with r_{12} and r_{1B} respectively. We see in all three plots no violation of the nonlocality bound, and the patterns are qualitatively the same as in Case II.

6.3.2 Configuration b

Here we plot S_ρ with T and r_{1B} in figs. 12a and 12b respectively. We notice the pattern of the nonlocality bound analogous to previously observed: in particular, S_ρ is always bounded by $S_{\text{CHSH}} = 2$. This again indicates the local nature of the correlations. Thus, the quantum state in Case II and III is local in Bell's sense but can produce non-classical correlations as the quantum discord is non-vanishing.

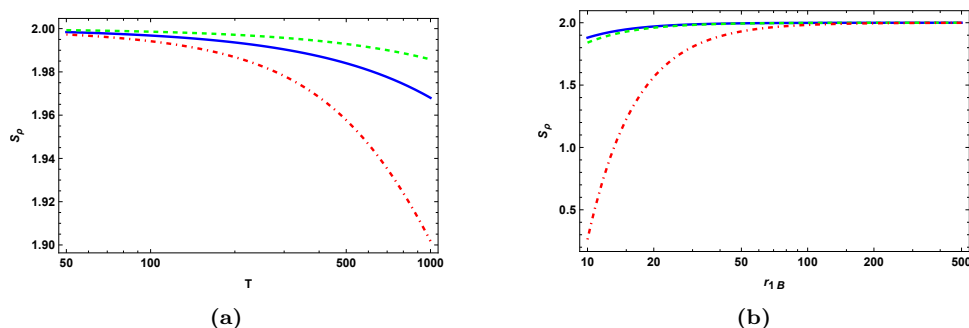


Figure 12: Quantum nonlocality S_ρ for ρ_{12}^f of (3.28): (a) S_ρ vs T for various r_{1B} $r_{1B} = 50$ (solid-blue), $r_{1B} = 75$ (green-dashed) and $r_{1B} = 100$ (red-dot-dashed). (b) S_ρ vs r_{1B} for various T : $T = 150$ (solid-blue), $T = 200$ (green-dashed) and $T = 250$ (red-dot-dashed).

In summary, in all three cases, the nonlocality bound is not violated for all the parameter ranges considered, and their patterns of S_ρ are qualitatively the same. Moreover, the qualitative results for all three RQI measures in all three cases are summarized in table 1. Based on this summary, we will discuss the contextual meanings of locality and quantumness in the next section.

	Case I	Case II	Case III
QFT	nonlocal and classical	nonlocal and quantum*	nonlocal and quantum*
RQI	local and classical	local and quantum	local and quantum
Entanglement harvesting	yes	no	yes

Table 1: Contextual meanings of locality and quantumness in quantum field theory (QFT) and relativistic quantum information (RQI). Recall that Case I: with Coulombic interaction between UDW qubits but no black hole; Case II: with a black hole but no Coloumbic interaction between UDW qubits; Case III: including both. Note that quantum* denotes the quantum effect attributed to the Hawking radiations.

7 Conclusion and Discussions: Contextual meanings of locality and quantumness

In this paper, we revisit the problem of the relativistic quantum information (RQI) for a pair of static UDW detectors in an ambient quantum field thermalized by a black hole. Instead of using the conventional approach, we adopt the effective field theory (EFT) by integrating out the ambient field and evaluating the reduced final states of UDW qubits analytically. With such neat results, we can calculate various RQI measures easily to characterize the entanglement, quantum correlation, and nonlocality bound, and the characteristics of the resultant RQI measures are summarized in table 1. These results will be difficult to obtain in the conventional approach with the master theory due to complicated numerical integration involving an infinite number of Matsubara thermal modes except for some gravitational backgrounds (such as BTZ black hole or de Sitter space) with closed forms of thermal Green functions. We find that our EFT results on the patterns of entanglement harvesting agree with the ones obtained by the master theory in the BTZ black hole background. Moreover, the EFT decomposes the effect of the mediator ambient quantum field into different interaction terms. We can then study the corresponding effect on RQI by each interaction term. Our effort in this work opens a new avenue for studying RQI problems using the EFT approach.

Besides, our results also raise some interesting issues on the contextual meaning of locality and quantumness. Locality and quantumness appear in quantum field theory and quantum information sciences; however, their meanings are contextual. We then compare the contextual meanings of locality first and then quantumness based on the summary in table 1.

In quantum field theory (QFT), locality means the interaction is local; in the relativistic context, it further requires the interaction to be causal, e.g., the influence domain mediated by the messenger fields is limited by the lightcone structure. On the other hand, in quantum information, locality means the Bell-like inequalities (in this work, we consider CHSH inequality) cannot be violated in Bell-type experiments, i.e., it means that the result of Bell-type experiments can be explained by some local hidden variables. However, such quantum nonlocality is not equivalent to quantum entanglement. The CHSH inequality is violated by the entangled pure states but not always by entangled mixed states.

Interestingly, we see some different contextual meanings of locality in our results. In Case I, the Coulombic forces between two static bodies are spooky and nonlocal. This is in contrast to the retarded electromagnetic (EM) force between freely moving charged bodies. The reason for this spooky/nonlocal Coulombic force is that the two charged bodies are held static so that the Coulomb potential is off-shell. In this case, we see nonzero quantum entanglement harvesting. That is, the Coulomb force can entangle two UDW qubits and thus seems nonlocal in both QFT and RQI contexts. However, when considering the Bell-type experiments, we see Case I does not violate the CHSH locality bound. Thus, we have different contextual meanings about locality. Moreover, in all three cases considered in this paper, the CHSH locality bound is not

violated. However, the entanglement measure for Case II is zero but nonzero for Case I and III. In summary, the local causality in the QFT context seems different from the locality bound of Bell-type experiments in the RQI context.

Now, we move to consider the contextual meanings of quantumness. In the QFT context, the quantumness usually means we go beyond the tree-level diagrams in the perturbative calculations. Thus, the Coulombic terms in the EFT can be considered the classical interaction, although we evolve the quantum states with the evolution operator induced by this interaction. Then, we estimate the pure quantum correlation of the reduced final states by the quantity of quantum discord in the RQI context, which gives the operational definition of the non-classical correlations. For Case I, we see that the quantum discord is zero. Thus, the QFT and RQI agree on the notion of quantumness. When a black hole with Hawking radiation appears, as in Case II and III, we see that quantum discord is nonvanishing. In this case, we can think that the Hawking radiation induced by the nontrivial quantum effect near the event horizon can create non-classical correlations between two UDW qubits. By this interpretation, the QFT in curved spacetime and the RQI again agree on the notion of quantumness but with a different physical origin from Case I.

One will expect to explore the contextual meanings of locality and quantumness when we apply the EFT approach to study RQI in more general settings. The results should help to classify some confusion due to the usage of the same terminologies in different contexts and hopefully end some contextual debates since the appearance of the EPR paper [54].

Acknowledgment

We thank Huan-Yu Ku for the helpful discussions. SM is grateful to Ignacio and Giorgos for their hospitality at Universidad Andres Bello and Universidad Adolfo Ibañez, respectively. The work of FLL is supported by Taiwan's NSTC with grant numbers 112-2112-M-003-006-MY3. The work of SM is supported by ANID FONDECYT Postdoctorado grant number 3240055.

References

- [1] A. Biggs and J. Maldacena, *Comparing the decoherence effects due to black holes versus ordinary matter*, [2405.02227](#).
- [2] A. Peres and D.R. Terno, *Quantum information and relativity theory*, *Rev. Mod. Phys.* **76** (2004) 93.
- [3] R.B. Mann and T.C. Ralph, *Relativistic quantum information*, *Classical and Quantum Gravity* **29** (2012) 220301.
- [4] E. Martin-Martinez, *Relativistic Quantum Information: developments in Quantum Information in general relativistic scenarios*, Ph.D. thesis, Waterloo U., 2011. [\[1106.0280\]](#).

- [5] P.M. Alsing and G.J. Milburn, *Lorentz invariance of entanglement*, 2002.
- [6] P.M. Alsing and G.J. Milburn, *Teleportation with a uniformly accelerated partner*, *Phys. Rev. Lett.* **91** (2003) 180404.
- [7] P.M. Alsing, D. McMahon and G.J. Milburn, *Teleportation in a non-inertial frame*, *Journal of Optics B: Quantum and Semiclassical Optics* **6** (2004) S834.
- [8] D.L. Danielson, G. Satishchandran and R.M. Wald, *Gravitationally mediated entanglement: Newtonian field versus gravitons*, *Phys. Rev. D* **105** (2022) 086001 [2112.10798].
- [9] D.L. Danielson, G. Satishchandran and R.M. Wald, *Killing horizons decohere quantum superpositions*, *Phys. Rev. D* **108** (2023) 025007 [2301.00026].
- [10] D.L. Danielson, G. Satishchandran and R.M. Wald, *Black holes decohere quantum superpositions*, *Int. J. Mod. Phys. D* **31** (2022) 2241003 [2205.06279].
- [11] S.E. Gralla and H. Wei, *Decoherence from horizons: General formulation and rotating black holes*, *Phys. Rev. D* **109** (2024) 065031 [2311.11461].
- [12] J. Wilson-Gerow, A. Dugad and Y. Chen, *Decoherence by warm horizons*, 2405.00804.
- [13] G. Salton, R.B. Mann and N.C. Menicucci, *Acceleration-assisted entanglement harvesting and rangefinding*, *New J. Phys.* **17** (2015) 035001 [1408.1395].
- [14] E. Martín-Martínez and B.C. Sanders, *Precise space–time positioning for entanglement harvesting*, *New J. Phys.* **18** (2016) 043031 [1508.01209].
- [15] E. Martín-Martínez, A.R.H. Smith and D.R. Terno, *Spacetime structure and vacuum entanglement*, *Phys. Rev. D* **93** (2016) 044001.
- [16] L.J. Henderson, R.A. Hennigar, R.B. Mann, A.R.H. Smith and J. Zhang, *Harvesting Entanglement from the Black Hole Vacuum*, *Class. Quant. Grav.* **35** (2018) 21LT02 [1712.10018].
- [17] S. Kukita and Y. Nambu, *Harvesting large scale entanglement in de Sitter space with multiple detectors*, *Entropy* **19** (2017) 449 [1708.01359].
- [18] T.R. Perche, B. Ragula and E. Martín-Martínez, *Harvesting entanglement from the gravitational vacuum*, *Phys. Rev. D* **108** (2023) 085025 [2210.14921].
- [19] K. Gallock-Yoshimura, E. Tjoa and R.B. Mann, *Harvesting entanglement with detectors freely falling into a black hole*, *Phys. Rev. D* **104** (2021) 025001.
- [20] D. Mendez-Avalos, L.J. Henderson, K. Gallock-Yoshimura and R.B. Mann, *Entanglement harvesting of three Unruh-DeWitt detectors*, *Gen. Rel. Grav.* **54** (2022) 87 [2206.11902].
- [21] F.-L. Lin and S. Mondal, *Entanglement harvesting and quantum discord of alpha vacua in de Sitter space*, *JHEP* **08** (2024) 159 [2406.19125].

- [22] W.D. Goldberger and I.Z. Rothstein, *An Effective field theory of gravity for extended objects*, *Phys. Rev. D* **73** (2006) 104029 [[hep-th/0409156](#)].
- [23] W.D. Goldberger, *Les Houches lectures on effective field theories and gravitational radiation*, in *Les Houches Summer School - Session 86: Particle Physics and Cosmology: The Fabric of Spacetime*, 1, 2007 [[hep-ph/0701129](#)].
- [24] R.A. Porto, *The effective field theorist's approach to gravitational dynamics*, *Phys. Rept.* **633** (2016) 1 [[1601.04914](#)].
- [25] T. Damour and A. Nagar, *Relativistic tidal properties of neutron stars*, *Phys. Rev. D* **80** (2009) 084035 [[0906.0096](#)].
- [26] T. Binnington and E. Poisson, *Relativistic theory of tidal Love numbers*, *Phys. Rev. D* **80** (2009) 084018 [[0906.1366](#)].
- [27] B. Kol and M. Smolkin, *Black hole stereotyping: Induced gravito-static polarization*, *JHEP* **02** (2012) 010 [[1110.3764](#)].
- [28] P. Charalambous, S. Dubovsky and M.M. Ivanov, *On the Vanishing of Love Numbers for Kerr Black Holes*, *JHEP* **05** (2021) 038 [[2102.08917](#)].
- [29] L. Hui, A. Joyce, R. Penco, L. Santoni and A.R. Solomon, *Ladder symmetries of black holes. Implications for love numbers and no-hair theorems*, *JCAP* **01** (2022) 032 [[2105.01069](#)].
- [30] O. Combaluzier-Szteinsznaider, L. Hui, L. Santoni, A.R. Solomon and S.S.C. Wong, *Symmetries of Vanishing Nonlinear Love Numbers of Schwarzschild Black Holes*, [2410.10952](#).
- [31] T. Appelquist and J. Carazzone, *Infrared Singularities and Massive Fields*, *Phys. Rev. D* **11** (1975) 2856.
- [32] S. Weinberg, *Effective Field Theory, Past and Future*, *PoS CD09* (2009) 001 [[0908.1964](#)].
- [33] M.M. Ivanov and Z. Zhou, *Revisiting the matching of black hole tidal responses: A systematic study of relativistic and logarithmic corrections*, *Phys. Rev. D* **107** (2023) 084030 [[2208.08459](#)].
- [34] M.M. Ivanov and Z. Zhou, *Vanishing of Black Hole Tidal Love Numbers from Scattering Amplitudes*, *Phys. Rev. Lett.* **130** (2023) 091403 [[2209.14324](#)].
- [35] M. Perry and M.J. Rodriguez, *Dynamical Love Numbers for Kerr Black Holes*, [2310.03660](#).
- [36] H. Ollivier and W.H. Zurek, *Quantum discord: A measure of the quantumness of correlations*, *Phys. Rev. Lett.* **88** (2001) 017901.

- [37] L. Henderson and V. Vedral, *Classical, quantum and total correlations*, *J. Phys. A* **34** (2001) 6899 [quant-ph/0105028].
- [38] R. Horodecki, P. Horodecki and M. Horodecki, *Violating bell inequality by mixed spin-1/2 states: necessary and sufficient condition*, *Physics Letters A* **200** (1995) 340.
- [39] N. Brunner, D. Cavalcanti, S. Pironio, V. Scarani and S. Wehner, *Bell nonlocality*, *Rev. Mod. Phys.* **86** (2014) 419 [1303.2849].
- [40] H. Buhrman, R. Cleve, S. Massar and R. de Wolf, *Nonlocality and communication complexity*, *Rev. Mod. Phys.* **82** (2010) 665.
- [41] A. Einstein, L. Infeld and B. Hoffmann, *The Gravitational equations and the problem of motion*, *Annals Math.* **39** (1938) 65.
- [42] R. Kubo, *Statistical mechanical theory of irreversible processes. 1. General theory and simple applications in magnetic and conduction problems*, *J. Phys. Soc. Jap.* **12** (1957) 570.
- [43] R. Kubo, M. Yokota and S. Nakajima, *Statistical-mechanical theory of irreversible processes. ii. response to thermal disturbance*, *Journal of the Physical Society of Japan* **12** (1957) 1203 [<https://doi.org/10.1143/JPSJ.12.1203>].
- [44] P.C. Martin and J. Schwinger, *Theory of many-particle systems. i*, *Phys. Rev.* **115** (1959) 1342.
- [45] W. Goldberger and I.Z. Rothstein, *Virtual hawking radiation*, *Phys. Rev. Lett.* **125** (2020) 211301.
- [46] R. Fabbri, *Scattering and absorption of electromagnetic waves by a Schwarzschild black hole*, *Phys. Rev. D* **12** (1975) 933.
- [47] D.N. Page, *Particle Emission Rates from a Black Hole: Massless Particles from an Uncharged, Nonrotating Hole*, *Phys. Rev. D* **13** (1976) 198.
- [48] J.-i. Koga, K. Maeda and G. Kimura, *Entanglement extracted from vacuum into accelerated Unruh-DeWitt detectors and energy conservation*, *Phys. Rev. D* **100** (2019) 065013 [1906.02843].
- [49] T. Yu and J.H. Eberly, *Evolution from entanglement to decoherence of bipartite mixed "x" states*, quant-ph/0503089.
- [50] W.K. Wootters, *Entanglement of formation of an arbitrary state of two qubits*, *Phys. Rev. Lett.* **80** (1998) 2245.
- [51] M. Ali, A.R.P. Rau and G. Alber, *Quantum discord for two-qubit x states*, *Phys. Rev. A* **81** (2010) 042105.

- [52] M.A. Yurischev, *On the quantum discord of general x states*, *Quantum Information Processing* **14** (2015) 3399.
- [53] Y. Huang, *Quantum discord for two-qubit x states: Analytical formula with very small worst-case error*, *Phys. Rev. A* **88** (2013) 014302.
- [54] A. Einstein, B. Podolsky and N. Rosen, *Can quantum-mechanical description of physical reality be considered complete?*, *Phys. Rev.* **47** (1935) 777.
- [55] E. Chitambar and G. Gour, *Quantum resource theories*, *Rev. Mod. Phys.* **91** (2019) 025001 [[1806.06107](#)].
- [56] C.H. Bennett, G. Brassard, C. Crepeau, R. Jozsa, A. Peres and W.K. Wootters, *Teleporting an unknown quantum state via dual classical and Einstein-Podolsky-Rosen channels*, *Phys. Rev. Lett.* **70** (1993) 1895.
- [57] C.H. Bennett and S.J. Wiesner, *Communication via one- and two-particle operators on Einstein-Podolsky-Rosen states*, *Phys. Rev. Lett.* **69** (1992) 2881.
- [58] B.S. Cirel'son, *Quantum generalizations of Bell's inequality*, *Letters in Mathematical Physics* **4** (1980) 93.
- [59] L.A. Khalfin and B.S. Tsirelson, *Quantum/classical correspondence in the light of bell's inequalities*, *Foundations of Physics* **22** (1992) 879.
- [60] D. Rohrlich and S. Popescu, *Nonlocality as an axiom for quantum theory*, in *60 Years of EPR: Workshop on the Foundations of Quantum Mechanics (In Honor of Nathan Rosen)*, 3, 1995 [[quant-ph/9508009](#)].
- [61] V. Capasso, D. Fortunato and F. Selleri, *Sensitive observables of quantum mechanics*, *Int. J. Theor. Phys.* **7** (1973) 319.
- [62] N. Gisin, *Bell's inequality holds for all non-product states*, *Physics Letters A* **154** (1991) 201.
- [63] D. Home and F. Selleri, *Bell's theorem and the EPR paradox*, *Riv. Nuovo Cim.* **14N9** (1991) 1.
- [64] R.F. Werner, *Quantum states with einstein-podolsky-rosen correlations admitting a hidden-variable model*, *Phys. Rev. A* **40** (1989) 4277.
- [65] F. Verstraete and M.M. Wolf, *Entanglement versus bell violations and their behavior under local filtering operations*, *Phys. Rev. Lett.* **89** (2002) 170401.